

This is the accepted manuscript made available via CHORUS. The article has been published as:

## Thermodynamic stability and unusual strength of ultra-incompressible rhenium nitrides

R. F. Zhang, Z. J. Lin, Ho-Kwang Mao, and Yusheng Zhao

Phys. Rev. B **83**, 060101 — Published 11 February 2011

DOI: [10.1103/PhysRevB.83.060101](https://doi.org/10.1103/PhysRevB.83.060101)

# Thermodynamic Stability and Unusual Strength of Ultra-incompressible Rhenium Nitrides

R. F. Zhang,<sup>1</sup> Z. J. Lin,<sup>2,3,\*</sup> Ho-Kwang Mao,<sup>2</sup> and Yusheng Zhao<sup>3,4</sup>

<sup>1</sup>*Theoretical division, Los Alamos National Laboratory, Los Alamos, New Mexico 87545, USA*

<sup>2</sup>*Geophysical Laboratory, Carnegie Institution of Washington, NW Washington, DC 20015, USA*

<sup>3</sup>*LANSCE–LC, Los Alamos National Laboratory, Los Alamos, New Mexico 87545, USA*

<sup>4</sup>*HiPSEC, University of Nevada, Las Vegas, Nevada 89154, USA*

## Abstract

We report the first comprehensive study of thermodynamic and mechanical properties as well as bond-deformation mechanism on newly discovered and ultra-incompressible  $\text{Re}_2\text{N}$  and  $\text{Re}_3\text{N}$ . The introduction of nitrogen into the rhenium lattice leads to thermodynamic instability in  $\text{Re}_2\text{N}$  at ambient conditions and enhanced incompressibility and strength for both rhenium nitrides. Rhenium nitrides, however, show substantially lower ideal shear strength than hard  $\text{ReB}_2$  and superhard c-BN, suggesting that they cannot be intrinsically superhard. An intriguing soft “ionic bond mediated plastic deformation” mechanism is revealed to underline the physical origin of their unusual mechanical strength. These results suggest a need of reformulating the design concept of intrinsically superhard transition metal nitrides, borides, and carbides.

\*Email: [zlin@ciw.edu](mailto:zlin@ciw.edu) or [zlin@lanl.gov](mailto:zlin@lanl.gov)

The introduction of light and covalent-bond forming elements into the transition metal (TM) lattices is expected to have profound influences on their chemical, mechanical, and electronic properties. Based on this prospect, recent design of new intrinsically superhard materials ( $H_v \geq 40$  GPa) has concentrated on light-element (e.g., B, C, N, and O) TM compounds with high elastic moduli,<sup>1-7</sup> such as OsB<sub>2</sub>,<sup>6</sup> ReB<sub>2</sub>,<sup>7</sup> PtN,<sup>8</sup> IrN<sub>2</sub>,<sup>9</sup> Re<sub>2</sub>C,<sup>10</sup> and PtC.<sup>11</sup> Although some of these ultra-incompressible compounds, such as OsB<sub>2</sub> and ReB<sub>2</sub>, are expected to be intrinsically superhard,<sup>6,7</sup> the experimentally determined load-invariant hardnesses are below 30 GPa.<sup>3</sup> These findings can be attributed to different physical origins of elastic moduli and hardness: elastic moduli describe the reversible, elastic deformation at small strains close to equilibrium; whereas plastic deformation occurs in an irreversible manner at atomic-level large shear strains where the electronic structure may undergo instability and transform to some phases with lower shear resistance. For example, OsB<sub>2</sub> possesses high zero-pressure elastic moduli but a low hardness, which was attributed to the presence of soft metallic Os-Os layers and hence its low ideal shear strengths.<sup>12</sup> Rhenium diboride was once thought to be intrinsically superhard,<sup>7</sup> but its load invariant hardness of <30 GPa<sup>7,13</sup> is much lower than that of c-BN (48 GPa in single crystal form<sup>14</sup>). At a finite shear, ReB<sub>2</sub> undergoes a series of electronic and structural instabilities due to the crystal field splitting of 5*d* electrons,<sup>13</sup> which limits its strength and hardness. Therefore, to be superhard, a solid must have a strong resistance against possible electronic and structural instabilities under extreme loading, which is accessible in stress-strain calculations based on density functional theory.<sup>12,13</sup> In addition, the ultra-incompressible compounds synthesized under high temperature and pressure (*P-T*) conditions can be stabilized by the impurity effect. For example, orthorhombic  $\eta$ -Ta<sub>2</sub>N<sub>3</sub>, synthesized under high *P-T* conditions by Zerr *et al.*<sup>15</sup>, displays

a hardness of 16 GPa (for a sample with a 10% porosity) and it is a highly promising candidate for applications as a hard and fracture-resistant material. First-principles calculations revealed that minor amount of oxygen incorporation played a remarkable role in stabilizing the orthorhombic  $\eta$ -Ta<sub>2</sub>N<sub>3</sub> structure.<sup>16</sup> Therefore, a thermodynamic consideration of stability is also warranted for future applications of hard/superhard materials. However, thermodynamic and mechanical stabilities have not been well explored for the design of new superhard materials. In this letter, we report a comprehensive study on the newly discovered rhenium nitrides (Re<sub>3</sub>N and Re<sub>2</sub>N) and use them as examples to underline the importance of these factors in the search for superhard materials.

Novel rhenium nitrides recently synthesized by Friedrich *et al.*<sup>17</sup> under high  $P$ - $T$  conditions, have stimulated great interest because of their ultra-incompressibility with bulk modulus of about 400 GPa. This value is comparable to that of superhard c-BN (around 400 GPa) and higher than that of hard ReB<sub>2</sub> (334-371 GPa).<sup>7,18</sup> Both nitrides can be potentially superhard based on the aforementioned design concept for intrinsically superhard compounds (i.e., high elastic moduli).<sup>5-7</sup> However, we show for the first time, that a combination of thermodynamic instability at ambient conditions, relatively low shear moduli and strengths, and soft “ionic” Re-N bonds inherently limits applications of Re<sub>3</sub>N and Re<sub>2</sub>N as superhard materials. These findings challenge the generally-accepted concept for the design of intrinsically superhard transition metal nitrides, borides, and carbides.<sup>5-7</sup> The unusual mechanical strengths are unveiled and a soft “ionic bond mediated plastic deformation” mechanism is proposed based on systematic analyses of atomic and electronic structures to a large strain.

Calculations were performed using the VASP code<sup>19</sup> with the generalized-gradient approximation proposed by Perdew and Wang for exchange-correlation functional. The integration in the Brillouin zone was employed using the Monkhorst-Pack scheme (9×9×9), energy cutoff of 600 eV, and tetrahedron method with Blöchl corrections for the energy calculation and Gaussian smearing for the stress calculations. Details of stress-strain calculations can be found in Refs. 20 and 21. The equilibrium structural parameters for both nitrides were obtained (space groups:  $P\bar{6}m2$  (No. 187) and  $P6_3/mmc$  (No. 194) for  $\text{Re}_3\text{N}$  and  $\text{Re}_2\text{N}$ , respectively) by fully relaxations of both lattice constants and internal atomic coordination. The optimized lattice constants are  $a=2.83$  Å ( $c=7.188$  Å) for  $\text{Re}_3\text{N}$  and  $a=2.86$  Å ( $c=9.88$  Å) for  $\text{Re}_2\text{N}$ , which are in good agreement with the experimental values:  $a=2.78$  Å ( $c=7.152$  Å) for  $\text{Re}_3\text{N}$  and  $a=2.83$  Å ( $c=9.88$  Å) for  $\text{Re}_2\text{N}$ .<sup>17</sup> The calculated atomic positions for  $\text{Re}_3\text{N}$  [Re(2/3, 1/3, 1/2), Re2(1/3, 2/3, 0.1988), N(2/3, 1/3, 1/2)] and  $\text{Re}_2\text{N}$  [Re(1/3, 2/3, 0.1055), N(2/3, 1/3, 1/4)] also agree well with the available experimental results.

To evaluate the thermodynamic feasibility of incorporating nitrogen into rhenium lattice, we calculated the formation enthalpy (energy) of both rhenium nitrides with respect to the metal Re and nitrogen at ambient conditions based on the following chemical reactions:  $4\text{Re}+\text{N}_2=2\text{Re}_2\text{N}$  and  $6\text{Re}+\text{N}_2=2\text{Re}_3\text{N}$ . The equilibrium N-N bond length in molecular nitrogen was calculated to be about 1.11 Å, in good agreement with the experimental value of 1.09 Å.<sup>22</sup> The calculated formation energies of rhenium nitrides show a slightly positive value of 0.02 eV/Re-atom for  $\text{Re}_2\text{N}$  and a negative value of -0.07 eV/Re-atom for  $\text{Re}_3\text{N}$ , indicating that  $\text{Re}_2\text{N}$  is thermodynamically unstable at ambient conditions. Such thermodynamic instability may

intrinsically limit its application as a superhard material, although  $\text{Re}_2\text{N}$  is quenchable from high  $P$ - $T$  conditions.<sup>17</sup>

The elastic stabilities, incompressibility, and rigidity of both nitrides are determined from the calculated elastic constants by applying a set of given strains with a finite variation between -0.02 and +0.02. Table I summarizes the second order elastic constants for Re,  $\text{Re}_3\text{N}$ , and  $\text{Re}_2\text{N}$  and compares them with those of hard  $\text{ReB}_2$  and superhard c-BN compounds. The calculated elastic constants of Re agree well with previous experimental and theoretical studies,<sup>23,24</sup> demonstrating the reliability of the present calculations. The mechanical stabilities of both rhenium nitrides satisfy the Born-Huang criterion for a hexagonal crystal [ $(C_{11} - C_{12}) > 0$ ,  $(C_{11} + C_{12} - 2C_{13}^2 / C_{33}) > 0$ ,  $C_{12} > 0$ ,  $C_{33} > 0$ ,  $C_{44} > 0$ ],<sup>25</sup> indicating both compounds are mechanical stable at ambient conditions. The derived Voigt bulk and shear moduli (see Table I) for  $\text{Re}_2\text{N}$  and  $\text{Re}_3\text{N}$  are both higher than those of Re, indicating that the introduction of nitrogen atoms into Re lattice enhances its incompressibility. The zero-pressure bulk moduli derived from Birch-Murnaghan equation of state for both nitrides, 397 and 401 GPa respectively for  $\text{Re}_3\text{N}$  and  $\text{Re}_2\text{N}$ , are in excellent agreement with the experimental values of 395 for  $\text{Re}_3\text{N}$  and 401 GPa for  $\text{Re}_2\text{N}$ .<sup>17</sup> However, it can be seen from Table I that the shear moduli of both rhenium nitrides are substantially lower than those of  $\text{ReB}_2$  and c-BN, suggesting a lower rigidity for rhenium nitrides.

The stress-strain relationships to large strains were calculated to determine the electronic and structural stabilities as well as ideal strength of Re,  $\text{Re}_3\text{N}$ , and  $\text{Re}_2\text{N}$ . Figure 1 shows the calculated stress-strain curves for  $\text{Re}_3\text{N}$  and  $\text{Re}_2\text{N}$ . The calculated anisotropic ideal strengths for Re,  $\text{Re}_3\text{N}$ , and  $\text{Re}_2\text{N}$  are also summarized in Table I and compared with those for hard  $\text{ReB}_2$ <sup>20</sup> and superhard c-BN<sup>21</sup>. The anisotropy ratios of tensile strengths ( $A = \sigma_{\max} : \sigma_{\min}$ ) for both

$\text{Re}_2\text{N}$  (2.11) and  $\text{Re}_3\text{N}$  (1.77) are much lower than that of Re (2.47), which indicates that rhenium nitrides display less anisotropic tensile strength than rhenium. On the other hand, the ideal shear strengths of  $\text{Re}_2\text{N}$  (12.4 GPa) and  $\text{Re}_3\text{N}$  (15.5 GPa) along the weakest (0001) $\langle 10\bar{1}0 \rangle$  slip system are higher than that of Re (9.9 GPa). However, the ideal shear strengths of both nitrides are much lower than those of  $\text{ReB}_2$  (34.4 GPa)<sup>20</sup> and c-BN<sup>21</sup> ( $\tau_{(111)[11\bar{2}]} = 58.3$  GPa), indicating much lower shear resistance or potential superhardness for both rhenium nitrides. In spite of their significantly higher bulk moduli, both rhenium nitrides are much weaker than h- $\text{ReB}_2$  and c-BN in terms of shear moduli and strengths. Thus, higher incompressibility does not necessarily guarantee higher shear resistance/hardness.

To gain insights into the effect of nitrogen incorporation, the electronic density of states (DOS) and bonding features of Re,  $\text{Re}_2\text{N}$ , and  $\text{Re}_3\text{N}$  are analyzed. Figure 2 shows the electronic DOS of Re,  $\text{Re}_3\text{N}$ , and  $\text{Re}_2\text{N}$ . All three phases show similar metallic bonding features because of finite DOS at the Fermi level ( $E_F$ ), which originate mostly from 5d electrons of Re. The DOS feature around  $E_F$  for the three phases, however, show different characteristics, in the sense that  $E_F$ , as determined by the spatial splitting of 5d orbitals of Re, locates at the bottom of a valley, a pseudogap, and the shoulder of a peak for Re,  $\text{Re}_3\text{N}$ , and  $\text{Re}_2\text{N}$ , respectively. The existence of pseudogap underneath  $E_F$  for  $\text{Re}_3\text{N}$  can be related to the electronic origin and is responsible for its higher shear strength and thermodynamic stability relative to  $\text{Re}_2\text{N}$ . These calculations are consistent with the experimental results.<sup>17</sup> In both nitrides, there is a strong hybridization between N 2p and Re 5d states, indicating a mixture of covalent and ionic bonding between Re and N atoms. To further demonstrate this bonding nature, we show in Figure 3 the distribution of

valence charge density difference (VCDD) on the  $(11\bar{2}0)$  plane of the two nitrides. Some bonding directionality is clearly revealed between Re and N, a typical feature of covalent/ionic bonding. Interestingly, the nearest-neighbor Re-Re distances along the  $c$  axis in both  $\text{Re}_2\text{N}$  (2.659 Å) and  $\text{Re}_3\text{N}$  (2.713 Å) are slightly shorter than that in Re metal (2.757 Å), owing to the charge transfer from nitrogen to rhenium within both nitrides. The Bader charge density analysis<sup>26</sup> further confirms the inhomogeneous charge transfer from N to Re atoms. The calculated Bader charges of different Re atoms are also indicated in the VCDD maps in Figure 3. It can be seen that the Re atoms in nitrides show inequivalence, which depends on the spatial geometry of different stacking of metallic Re layers. This difference leads to various charge transfer and hence ionic contribution to the Re-N bonding. The Re layer neighboring the nitrogen layer contributes mostly to the charge transfer, i.e., so-called “ionicity”.

Finally, the topological bond structures of both nitrides before and after the shear instability were analyzed to understand the deformation mechanism. Figure 4 shows the topological structures for both nitrides at equilibrium and after lattice instability under  $(0001)\langle 10\bar{1}0 \rangle$  shear deformation (about 15.9% and 15.8% for  $\text{Re}_3\text{N}$  and  $\text{Re}_2\text{N}$ , respectively). The “ionic” Re-N bonds (as indicated by blue arrowheads) become unstable (“breaking”) at critical shear strains for  $\text{Re}_3\text{N}$  and  $\text{Re}_2\text{N}$ , which limits the achievable strengths of both nitrides. The instability of Re-N bonds under shear deformation for  $\text{Re}_3\text{N}$  and  $\text{Re}_2\text{N}$  can be attributed to the spatial splitting of  $5d$  orbitals as demonstrated by the valence charge distribution (not shown for brevity). The weakening of three dimensional Re-N bonds can also be correlated to the significant charge transfer (“ionicity”) as shown in Fig. 3, which is more significant in  $\text{Re}_2\text{N}$  than that in  $\text{Re}_3\text{N}$ . Such results emphasize



the importance of forming three dimensional covalent bond networks for the design of new superhard compounds.

In summary, we carried out systematic first-principles calculations on thermodynamic and mechanical stabilities, elastic properties, and ideal strengths for recently discovered  $\text{Re}_3\text{N}$  and  $\text{Re}_2\text{N}$ . The introduction of nitrogen into the rhenium lattice enhances incompressibility, elastic stiffness, and ideal strength of both nitrides due to the formation of covalent/ionic Re-N bonds and the strengthening of Re-Re bonds relative to that in Re metal. However, because of their thermodynamic instability and significant lower ideal shear strength of rhenium nitrides than those of hard  $\text{ReB}_2$  and superhard c-BN, both nitrides cannot be intrinsically superhard. Detailed analyses of the deformed atomic and electronic structures reveal that the weak “ionic” Re-N bonds limit their achievable strength and are also responsible for their unusual mechanical properties. The present study highlights the importance of thermodynamic stability, bonding feature, and bond deformation mechanism in the design of and search for intrinsically hard/superhard materials.

## **Acknowledgment**

We thank Drs. Russell J. Hemley, Ronald Cohen, and Jianzhong Zhang for comments on this paper. We would also like to thank Prof. S. Veprek for suggestion and support and Prof. G. Kresse for valuable advice for the application of VASP. Work at Los Alamos is supported by Los Alamos National Security LLC under DOE contact DEAC52-06NA25396. This work is supported as part of the EFree, an Energy Frontier Research Center funded by the DOE, Office of Science and Basic Energy Sciences (DE-SC0001057). UNLV HiPSEC is supported by the US Department of Energy, NNSA, under agreement No. DEFC52-06NA26274.

## References

- <sup>1</sup>A. Y. Liu and M. L. Cohen, *Science* **245**, 841 (1989).
- <sup>2</sup>D. M. Teter and R. J. Hemley, *Science* **271**, 53 (1996).
- <sup>3</sup>S. Veprek, *J. Vac. Sci. Technol. A* **17**, 2401 (1999).
- <sup>4</sup>V. V. Brazhkin, A. G. Lyapin, and R. J. Hemley, *Philos. Mag. A* **82**, 231 (2002).
- <sup>5</sup>R. B. Kaner, J. J. Gilman, and S. H. Tolbert, *Science* **308**, 1268 (2005).
- <sup>6</sup>R. W. Cumberland, M. B. Weinberger, J. J. Gilman, S. M. Clark, S. H. Tolbert, and R. B. Kaner, *J. Am. Chem. Soc.* **127** (2005).
- <sup>7</sup>H. Y. Chung, M. B. Weinberger, J. B. Levine, A. Kavner, J. M. Yang, S. H. Tolbert, and R. B. Kaner, *Science* **316**, 436 (2007).
- <sup>8</sup>E. Gregoryanz, C. Sanloup, M. Somayazulu, J. Badro, G. Fiquet, H. K. Mao, and R. J. Hemley, *Nat. Mater.* **3**, 294 (2004).
- <sup>9</sup>A. F. Young, C. Sanloup, E. Gregoryanz, S. Scandolo, R. J. Hemley, and H. K. Mao, *Phys. Rev. Lett.* **96**, 155501 (2006).
- <sup>10</sup>E. A. Juarez-Arellano, B. Winkler, A. Friedrich, D. J. Wilson, M. Koch-Müller, K. Knorr, S. C. Vogel, J. J. Wall, H. Reiche, W. Crichton, M. Ortega-Aviles, and M. Avalos-Borja, *Z. Kristallogr.* **223**, 492 (2008).
- <sup>11</sup>S. Ono, T. Kikegawa, and Y. Ohishi, *Solid State Commun.* **133**, 55 (2005).
- <sup>12</sup>J. Yang, H. Sun, and C. F. Chen, *J. Am. Chem. Soc.* **130**, 7200 (2008).
- <sup>13</sup>R. F. Zhang, D. Legut, R. Niewa, A. S. Argon, and S. Veprek, *Phys. Rev. B* **82**, 104104 (2010).
- <sup>14</sup>D. W. He, Y. S. Zhao, L. Daemen, J. Qian, T. D. Shen, and T. W. Zerda, *Appl. Phys. Lett.* **81**, 643 (2002).

- <sup>15</sup>A. Zerr, G. Miehe, J. W. Li, D. A. Dzivenko, V. K. Bulatov, H. Höfer, N. Bolfan-Casanova, M. Fialin, G. Brey, T. Watanabe, and M. Yoshimura, *Adv. Funct. Mater.* **19**, 2282 (2009).
- <sup>16</sup>C. Jiang, Z. J. Lin, and Y. S. Zhao, *Phys. Rev. Lett.* **103**, 185501 (2009).
- <sup>17</sup>A. Friedrich, B. Winkler, L. Bayarjargal, W. Morgenroth, E. A. Juarez-Arellano, V. Milman, K. Refson, M. Kunz, and K. Chen, *Phys. Rev. Lett.* **105**, 085504 (2010).
- <sup>18</sup>Y. J. Wang, J. Z. Zhang, L. L. Daemen, Z. J. Lin, Y. S. Zhao, and L. P. Wang, *Phys. Rev. B* **78**, 224106 (2008).
- <sup>19</sup>G. Kresse and J. Furthmüller, *Comput. Mater. Sci.* **6**, 15 (1996).
- <sup>20</sup>R. F. Zhang, S. Veprek, and A. S. Argon, *Appl. Phys. Lett.* **91**, 201914 (2007).
- <sup>21</sup>R. F. Zhang, S. Veprek, and A. S. Argon, *Phys. Rev. B* **77**, 172103 (2008).
- <sup>22</sup>K. W. Whitten, R. E. Davis, M. L. Peck, and G. G. Stanley, *Chemistry*, ninth edition, page 337, (Cengage Learning 2009).
- <sup>23</sup>M. H. Manghnani, K. Katahara, and E. S. Fisher, *Phys. Rev. B* **9**, 1421 (1974).
- <sup>24</sup>G. Steinle-Neumann, L. Stixrude, and R. E. Cohen, *Phys. Rev. B*, **60**, 791 (1999).
- <sup>25</sup>M. Born and K. Huang, *Dynamical Theory of Crystal Lattice* (Oxford University Press, Oxford, 1954).
- <sup>26</sup>R. F.W. Bader, *Atoms in Molecules-A Quantum Theory* (Oxford University Press, Oxford, 1990).

**TABLE I.** Single-crystal elastic constants  $c_{ij}$  (in GPa), the Voigt bulk modulus  $B_V$ , shear modulus  $G_V$ , and ideal strength (minimum tensile strength  $\sigma_{\min}$  and shear strength  $\tau_{\min}$ , as well as maximum ideal tensile strength  $\sigma_{\max}$ ) of Re,  $\text{Re}_3\text{N}$  and  $\text{Re}_2\text{N}$  calculated by first principles methods. Previous experimental and theoretical results for Re<sup>23,24</sup> and calculated results for h- $\text{ReB}_2$ <sup>20</sup> and c-BN<sup>21</sup> are also included for comparison.

Material	$c_{11}$	$c_{33}$	$c_{12}$	$c_{13}$	$c_{44}$	$c_{66}$	$B_V$	$G_V$	$\sigma_{\max}$	$\sigma_{\min}$	$\tau_{\min}$
Re	594	654	288	227	161	153	370	168	$\sigma_{\langle 0001 \rangle} = 53.8$	$\sigma_{\langle \bar{1}2\bar{1}0 \rangle} = 21.8$	$\tau_{(0001)\langle 10\bar{1}0 \rangle} = 9.9$
Re <sup>23</sup>	618	683	275	206	161	171					
Re <sup>24</sup>	640	695	280	220	170	180					
$\text{Re}_2\text{N}$	618	737	207	306	159	206	401	182	$\sigma_{\langle 0001 \rangle} = 60.0$	$\sigma_{\langle \bar{1}2\bar{1}0 \rangle} = 28.5$	$\tau_{(0001)\langle 10\bar{1}0 \rangle} = 12.4$
$\text{Re}_3\text{N}$	649	745	212	276	184	219	397	203	$\sigma_{\langle 0001 \rangle} = 61.1$	$\sigma_{\langle \bar{1}2\bar{1}0 \rangle} = 34.5$	$\tau_{(0001)\langle 10\bar{1}0 \rangle} = 15.5$
$\text{ReB}_2$ <sup>20</sup>	631	1015	158	134	257		348	274	$\sigma_{\langle 0001 \rangle} = 93.2$	$\sigma_{\langle \bar{1}2\bar{1}0 \rangle} = 58.5$	$\tau_{(0001)\langle 10\bar{1}0 \rangle} = 34.4$
c-BN <sup>21</sup>	786		172		445		376	390	$\sigma_{\langle 1\bar{1}0 \rangle} = 84.1$	$\sigma_{\langle 111 \rangle} = 55.3$	$\tau_{(111)\langle 11\bar{2} \rangle} = 58.3$

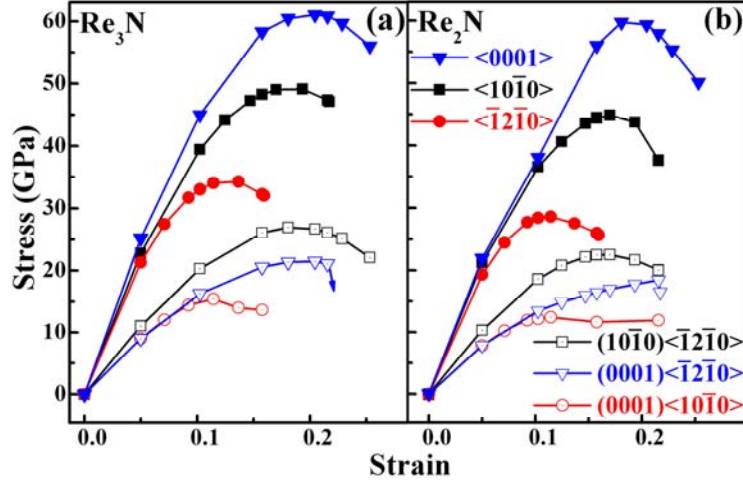


**FIG. 1** (Color online). Stress-strain relationships for (a)  $\text{Re}_3\text{N}$  and (b)  $\text{Re}_2\text{N}$  calculated by *ab initio* density functional theory.

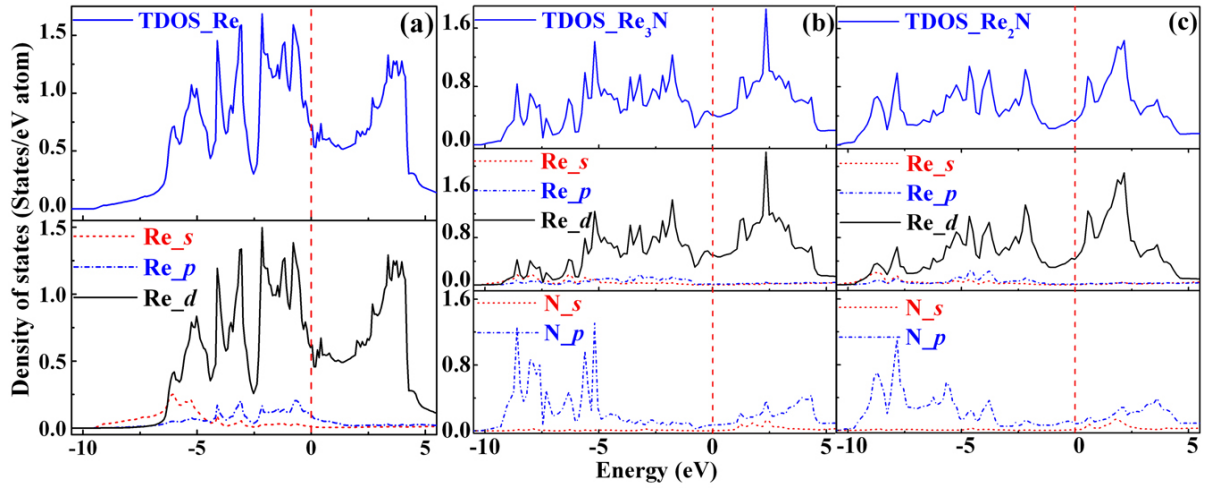


**FIG. 2** (Color online). Total and partial electronic density of states of (a) Re, (b)  $\text{Re}_3\text{N}$ , and (c)  $\text{Re}_2\text{N}$ . The vertical dashed lines indicate the Fermi levels.

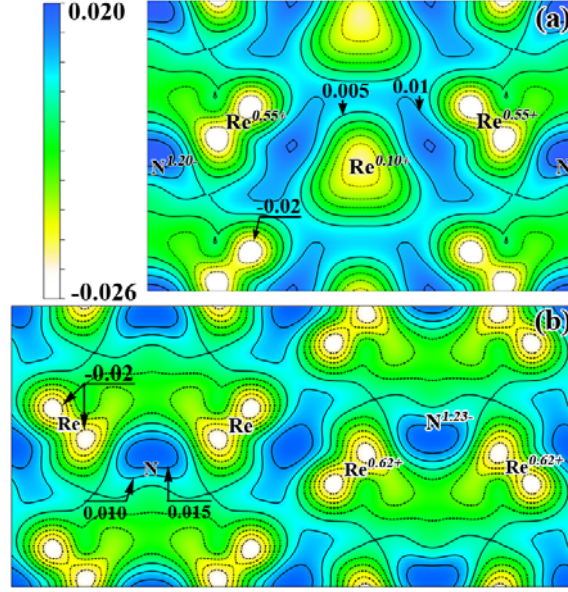


**FIG. 3** (color online). Maps of the valence charge density differences (VCDD) on the  $(11\bar{2}0)$  plane for (a)  $\text{Re}_3\text{N}$  and (b)  $\text{Re}_2\text{N}$ . The scale runs from 0.20 (blue) to -0.26 electrons/ $\text{Bohr}^3$  (white). The Bader charges are indicated by italic font.

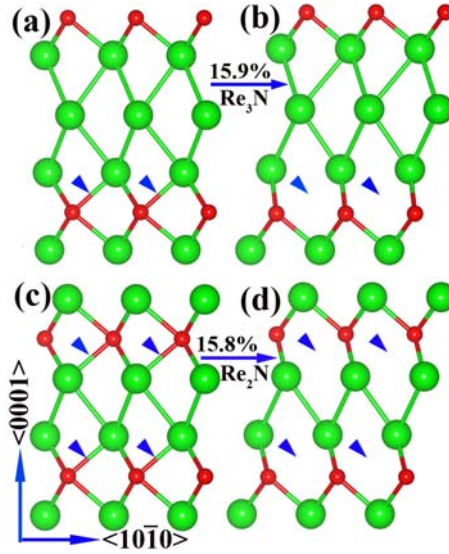


**FIG. 4** (color online). Topological bond structures at equilibrium for (a)  $\text{Re}_3\text{N}$  and (c)  $\text{Re}_2\text{N}$ , and those after the lattice instability for (b)  $\text{Re}_3\text{N}$  and (d)  $\text{Re}_2\text{N}$ . The large and small spheres represent Re and N atoms, respectively. The blue arrowheads indicate the instability of Re-N bonds upon shearing.